SAND REPORT

SAND2008-7053
Unlimited Release
October 2008

Capturing CO_2 via reactions in nanopores

Kevin Leung, Tina M. Nenoff, Louise J. Criscenti, Z. Tang, and J. H. Dong

Prepared by
Sandia National Laboratories
Albuquerque, New Mexico 87185 and Livermore, California 94550

Sandia is a multiprogram laboratory operated by Sandia Corporation, a Lockheed Martin Company, for the United States Department of Energy under Contract DE-AC04-94AL85000.

Issued by Sandia National Laboratories, operated for the United States Department of Energy by Sandia Corporation.

Available to DOE and DOE contractors from
U.S. Department of Energy
Office of Scientific and Technical Information
P.O. Box 62
Oak Ridge, TN 37831

Telephone:	(865) 576-8401
Facsimile:	(865) 576-5728
E-Mail:	reports@adonis.osti.gov
Online ordering:	http://www.doe.gov/bridge

Available to the public from
U.S. Department of Commerce
National Technical Information Service
5285 Port Royal Rd
Springfield, VA 22161

Telephone:	(800) 553-6847
Facsimile:	(703) 605-6900
E-Mail:	orders@ntis.fedworld.gov
Online ordering:	http://www.ntis.gov/ordering.htm

SAND2008-7053
Unlimited Release
Printed October 2008

Capturing CO_2 via reactions in nanopores

Kevin Leung and Tina M. Nenoff
Surface and Interface Sciences (01114)

Louise J. Criscenti, Geochemistry (06316)

Sandia National Laboratories
P.O. Box 5800
Albuquerque, NM 87185

Z. Tang and J. H. Dong
University of Cincinnati

Acknowledgement

We thank Ida Nielsen for helping write parts of the original LDRD proposal. We also thank Ellen Stechel and Christopher Daub for useful discussions.

Contents

Figures

Tables

Capturing CO_2 via reactions in nanopores

Abstract

This one-year exploratory LDRD aims to provide fundamental understanding of the mechanism of CO_2 scrubbing platforms that will reduce green house gas emission and mitigate the effect of climate change. The project builds on the team member's expertise developed in previous LDRD projects to study the capture or preferential retention of CO_2 in nanoporous membranes and on metal oxide surfaces. We apply Density Functional Theory and *ab initio* molecular dynamics techniques to model the binding of CO_2 on MgO and CaO (100) surfaces and inside water-filled, amine group functionalized silica nanopores. The results elucidate the mechanisms of CO_2 trapping and clarify some confusion in the literature. Our work identifies key future calculations that will have the greatest impact on CO_2 capture technologies, and provides guidance to science-based design of platforms that can separate the green house gas CO_2 from power plant exhaust or even from the atmosphere. Experimentally, we modify commercial MFI zeolite membranes and find that they preferentially transmit H_2 over CO_2 by a factor of 34. Since zeolite has potential catalytic capability to crack hydrocarbons into CO_2 and H_2, this finding paves the way for zeolite membranes that can convert biofuel into H_2 and separate the products all in one step.

1 Introduction

The continued use of carbon fuels is unavoidable for the near to mid term, and carbon sequestration has been identified as a key technology option for greenhouse gas emissions abatement in the Department of Energy's Carbon Sequestration Technology Road Map And Program Plan, 2006. As such, the work described in this report has the potential to build a critical capability in new core mission areas for both Sandia and the Department of Energy. The capture of CO_2 from combustion exhaust (or even from the atmosphere) is an essential component of carbon sequestration. Post-combustion capture entails the trapping of relatively pure CO_2 from an exhaust stream containing a mixture of gaseous products[1]. Current CO_2 capture technologies employ a Solvay-like process, the first step of which involves dissolving CO_2 in an alkaline solution[2]. The associated operation costs are high, however, and application of currently existing CO_2 sequestration technologies in power plants can increase power production costs by as much as 50%[3], with CO_2 capture alone accounting for an estimated three-fourths of this increase[4, 5]. We here report on modeling of novel approachs for CO_2 capture mechanisms based on (1) solubilizing CO_2 using water-filled inorganic nanopores; (2) using metal oxide substrates to bind to CO_2. The former is alternative way to catalyze the conversion of CO_2 to carbonic acid in water while the latter traps CO_2 in dry conditions. These approaches have the potential to greatly reduce the cost of CO_2 capture. We apply state-of-the-art *ab initio* molecular dynamics (AIMD) techniques to understand CO_2 reactions in water inside nanopores, and we will identify how pore properties, such as the nano-confinement and the presence of specific functional groups (e.g., amine groups which have already been incorporated in some synthetic nanopores[6, 7]) may be tailored to facilitate the reaction. Density Functional Theory (DFT) methods are applied to investigate the binding of isolated and monolayer CO_2 on MgO and CaO (100) surfaces. Our work takes advantage of unique capabilities provided by Sandia's massively parallel computing platforms, and leverages promising results from ongoing LDRD work[8, 9, 10] on the interactions between water and synthetic nanopores.

One clear conclusion that emerges from our basic science study of CO_2 binding with substrates is the fact that CO_2 is a stable, chemically fairly inert molecule. Strong CO_2 adsorption (or "chemisorption") is found to require as its first step the nucleophilic attack on the carbon atom in all cases, *not* weak-hydrogen bonding to the CO_2 oxygen site. Enhancing the binding energies or free energies between CO_2 and prospective material substrates will be particularly crucial for capture of CO_2 from the atmosphere, which is an active and ambitious research area that has generated much interest at Sandia.

Capturing CO_2 also provides the option to convert this climate-change inducing combustion waste product, through chemical reduction, into useful transportation fuel precursors such as carbon monoxide, formic acid, and polyatomic carbon-containing molecules. For example, CO_2 capture may be a critical step for supplying the CO_2 feedstock for a current Sandia LDRD "Sunshine to Petrol" grand challenge LDRD project that employs solar energy for catalytic reduction of CO_2 to carbon monoxide[11]. Our modeling work on CO_2 described herein has attracted substantial interest, and forms a large part of the modeling component of a DARPA and an Energy Frontier Research Center (EFRC) BES proposal being put together by Ellen Stechel at Sandia.

Finally, we also perform experimental investigation of modified commercial MFI zeolite membranes that selectively transmit H_2 over CO_2. These platforms have functionalities that can be integrated with CO_2 photochemical reduction cells. This work is performed in collaboration with the university of Cincinnitti, and leverages Tina Nenoff's expertise in zeolite separation membranes[12, 13].

2 Zeolite membranes for separating CO_2 from H_2

This part of the LDRD is a collaborative experimental effort between Tina Nenoff (01114) and Professor Dong Junhang at the University of Cincinnitti. In our previous work, we demonstrated that siliceous MFI zeolite membrane synthesized by in-situ method showed a dramatic improvement in the separation of H_2/CO_2 mixture after the membrane was on-stream modified with MDES. The effect of modification on MFI zeolite with very high Si/Al ratio (1050) investigated in this work has shown that MDES precursor can be successfully deposited and decomposed on the internal surface of such zeolite by means of operating at a reducing atmosphere. We conducted this membrane modification on MFI membrane with Si/Al ratio $>$ 1000 (for high temperature stability). The results are summarized below (see also Table 1).

The fresh MFI membrane showed a H_2/CO_2 separation factor of 3.8 at 450^{o}C, indicating a Knudsen diffusion mechanism. While the feed stream (equimolar CO_2 + H_2) was kept online, the modification was started at 150^{o}C with a heating rate of 0.5^{o}C/min until 450^{o}C. Separation of equimolar H_2/CO_2 dry gas mixture in the modified membrane was monitored by an on-line GS/MS system. As shown in Fig. 1, the separation factor increased with the modification temperature. The separation factor on the modified membrane reached $\sim$28 at 450^{o}C for a H_2/CO_2 equimolar mixture during the first cycle of modification. When the modification was stopped the separation factor dropped to below 20. The separation factor further increased to $\sim$ 60 during the second modification at 450^{o}C, and remained above 30 after the second modification was finished (Fig. 1). Gas pressure at the feed side was set to 15 psi (feed flow: 22.5+22.5 ml/min). Helium was used as the sweeping gas in this experiment. These results showed that the separation performance was improved dramatically when the second modification was employed. However, the permeance of H_2 decreased from 2.7×10^{-7} mol $m^{-2}s^{-1}Pa^{-1}$ to 0.8×10^{-7}. These findings will be described in detail in a publication under preparation[14].

H_2/CO_2 ratio	enhancement factor
after modification	3.8
1st round	15
2nd round	34

Table 1. The H_2/CO_2 enhancement ratio observed with successive rounds of modification of MFI zeolite membranes. The measurements were performed at T=450^{o}C.

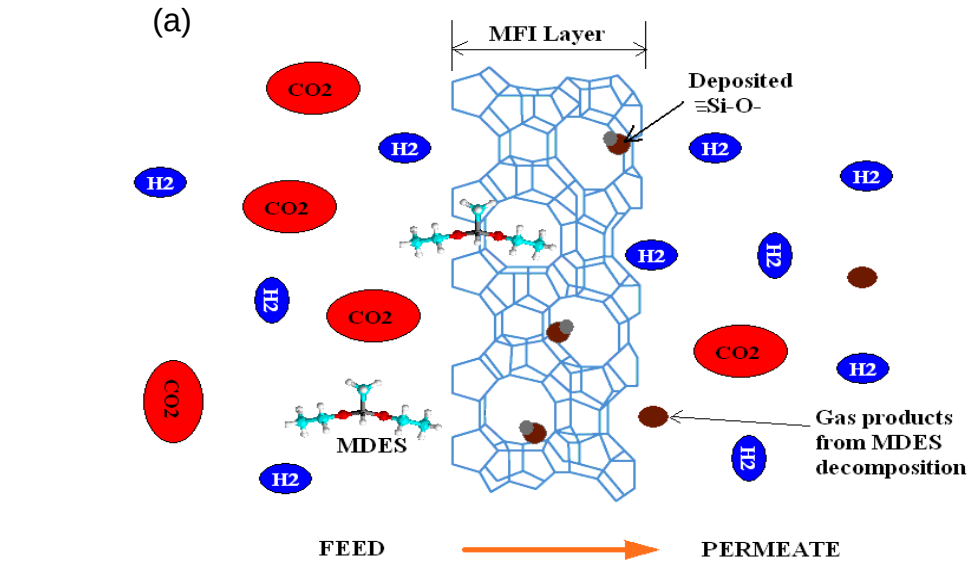

Figure 1. (a) Illustration of the MDES modified MFI zeolite membrane. (b) Temperature dependence and effect of MDES modification on H_2/CO_2 separation performance of zeolite membranes.

3 Adsorption of CO_2 on MgO and CaO (100) surfaces

A. Introduction

We perform DFT studies of CO_2 adsorption on MgO and CaO (100) surfaces. Previous thermodynamic measurements at Sandia and elsewhere (e.g., Ref. [15, 16], Fig. 2) have identified these oxides as promising candidates for use as CO_2 capture substrates. Here the metric of success is not limited to the CO_2 trapping efficiency ϕ during the first pass of CO_2 through the system. Instead, repeated thermal cycles that induces CO_2 release to regenerate the oxide material for reuse is envisioned. Thus, a relatively low temperature needed to drive off CO_2 is a desirable feature, as is the stability of ϕ as heating/cooling cycling proceeds. Heat treatment, as well as the repeated chemical reactions with CO_2, will change the morphology of the oxide surfaces as well as its domain/grain size, and will affect the CO_2 capture ability. Our work, which focuses on the adsorption of isolated and monolayer CO_2 on pristine (100) MgO and CaO surfaces, is a first step towards elucidating the scientific basis of the CO_2 capture performance observed in experiments[15, 16]. As will be shown, our calculations reported herein already serve to clarify some confusion in the literature, and they help lay the foundation for future modeling work in this area.

B. Methods

Density functional theory (DFT) calculations apply the VASP code[17], projected augmented wave (PAW) pseudopotentials[18, 19], the LDA and PBE[20] exchange correlation functionals, a 400 eV plane wave energy cutoff for wavefunctions, and a 10^{-4} eV convergence criterion. Simulation cells have a slab geometry and contain 3 layers of MgO or CaO atoms and is 18 Å in the direction normal to the periodically replicated MgO/CaO (100) surface; in other words, there is a vacuum layer of ∼12 Å. See Fig. 3. The lattice constant of the MgO primitive cell is determined to be 4.167 Å (LDA), 4.258 Å and (PBE), implying that the nearest neighbor Mg-O distance is 2.084 Å and 2.129 Å respectively, while the LDA lattice constant for CaO is 4.722 Å. The lateral dimensions of the simulation cells are adjusted according to these lattice constants.

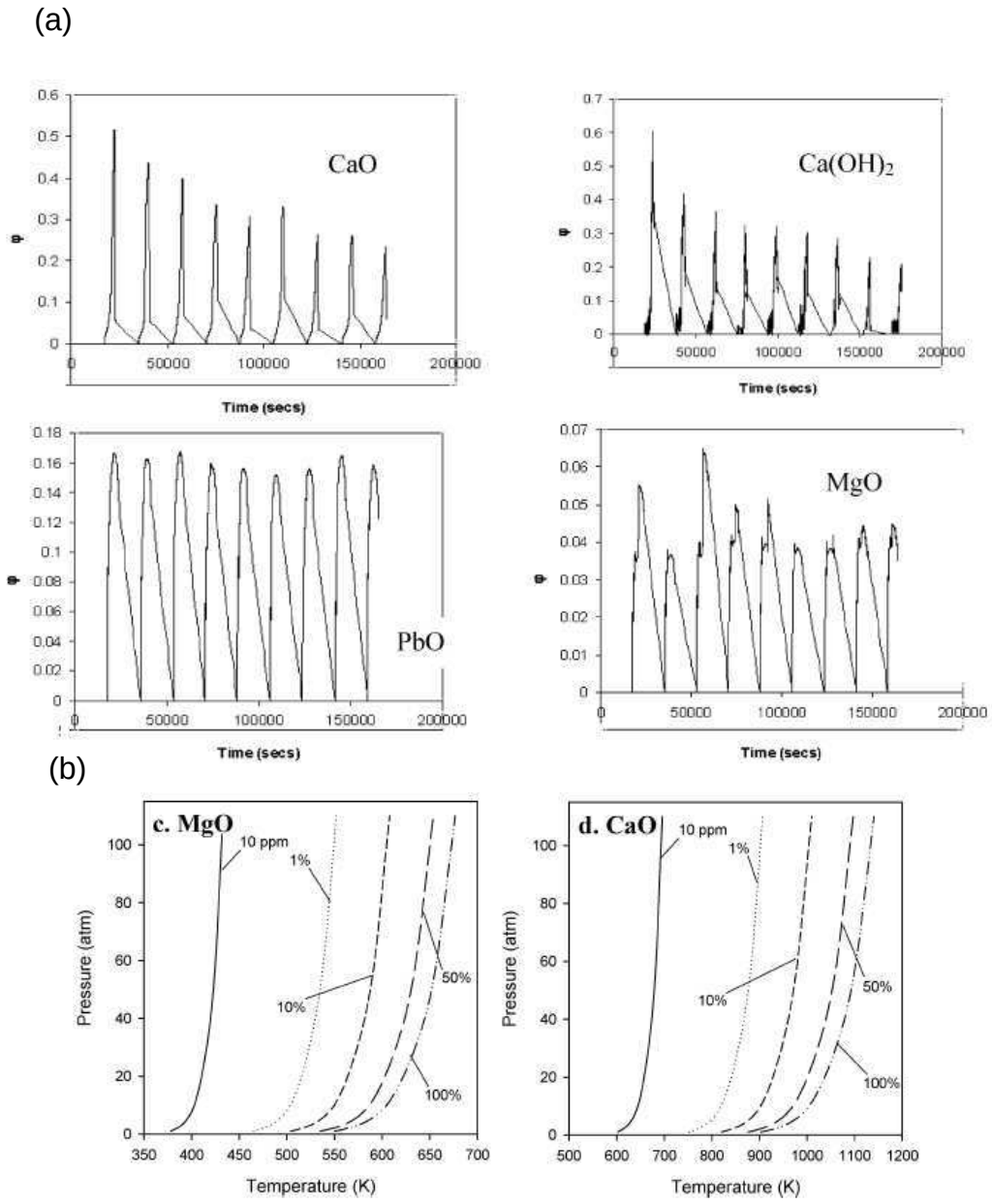

Figure 2. CO_2 capture fraction ϕ as a function of time, as heating/cooling cycles proceed. (b) Temperature-pressure phase diagram. Adapted from Ref. [15].

C. Isolated CO_2 on MgO and CaO

Isolated CO_2 is found to adsorb most favorably when its carbon atom sits on top of a MgO oxygen site. The two CO_2 oxygen atoms are aligned in the (010) or the equivalent (001) direction, thus allowing these partially negatively charged atoms to reside atop the partially positively charged metal atoms (Fig. 3a). The LDA (PBE) binding energy on MgO is 1.05 eV (0.39 eV). The LDA (PBE) O_{MgO}-C bond distance ais 1.44 Å (1.46 Å). CO_2 exhibits a bent geometry, with the C-O bonds lengthened from 1.17 (1.18) Å to 1.24 (1.26) Å. The LDA O-C-O angles are 117, 117, and 134^o, respectively. These values indicate that CO_2 has chemisorbed onto the MgO surface, forming a nascent bicarbonate ion-like structure; the configuration is reminiscent of OH^- nucleuophilic attack on the carbon atom in liquid water[9].

CO_2 chemisorption on CaO exhibits qualitatively similar features. The LDA binding energy is 2.02 eV while the C-O_{CaO} bond length is 1.395 Å. This distance is smaller than that for chemisorbed CO_2 on MgO, indicating a stronger C-O bond and is consistent with the much larger binding energy. We have not applied the PBE functional to CaO because LDA appears to give more accurate dispersion forces in these systems.

As will be discussed shortly, it is also worth examining a less favorable mode of adsorption where the carbon atom sits on top of the hollow site formed by two surface O and two Mg atoms. The two CO_2 oxygen atoms protrude along the (011) or (01$\bar{1}$) directions to attain a favorable proximity to Mg atoms. The CO_2 molecule remains linear with no significant bending of the CO_2 O-C-O structure (90^o, 90^o, and 180^o O-C-O angles), and it lies 2.28 (2.55) Å above the MgO surface. The LDA (PBE) binding energy is 0.49 (0.09) eV. These values clearly suggest CO_2 physisorption. The difference in LDA and PBE binding energies arises from the gross underestimation of dispersion forces predicted by the PBE functional. On the other hand, LDA often predicts reasonable dispersion forces, although the good agreement is not well understood and may be fortuitous. If one assumes the 0.4 eV difference between LDA and PBE is completely due to the magnitude of dispersion forces, then these van der Waals forces also largely explain the 0.65 eV difference in binding energies predicted by LDA and PBE for chemisorbed CO_2 after one takes into account that the distance between CO_2 and MgO surface is much smaller ($\sim$1.4 Å) in the case of chemisorption.

In the literature, where CO_2-MgO binding energies have been reported, it appears that erroneous assumptions have been made. For example, using the same VASP code and the LDA functional, Schneider reported a much lower binding energy[21]. The reason is that the geometry assumed therein is metastable, rotated by 45^o about the normal to the surface, which lessens the favorable electrostatic interactions between the CO_2 oxygen atoms and MgO surface metal sites. Quantum chemistry calcula-

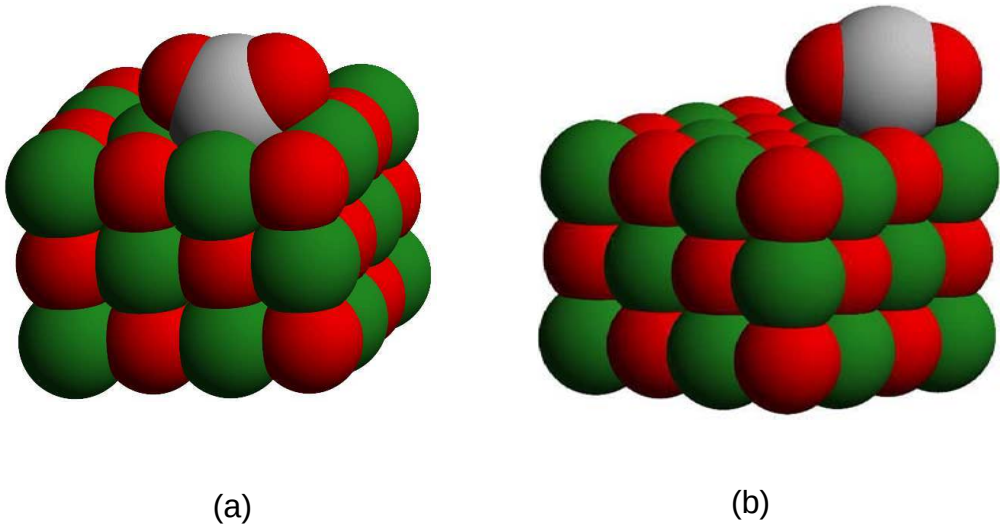

Figure 3. Two configurations of isolated CO_2 adsorption on a MgO (100) surface. (a) CO_2 chemisorbed on top of a surface oxygen atom. (b) CO_2 physisorbed on a hollow site formed by two Mg and two O atoms. Green, red, and gray spheres represent Mg/Ca, O, and C, respectively.

tions using cluster models and Hartree-Fock level of theory have suggested that the chemisorbed of CO_2 adsorption on the MgO (100) surface is metastable compared to infinite separation of the two species[22]. This erroneous prediction likely arises from the lack of proper treatment of electron correlations in the Hartree-Fock formalism.

D. Monolayer CO_2 on MgO and CaO

Next we consider a monolayer of CO_2 on MgO and CaO (100) surfaces. We find that the MgO lattice constant is too small for all CO_2 molecules present to chemisorb on to MgO oxygen sites. Such a configuration is found to yield substantial repulsion between neighboring CO_2 molecules and a net *repulsive* (negative) binding energy. The most favorable configuration occurs when all CO_2 are physisorbed diagonally on the MgO surface, which avoids steric hindrance between CO_2. See Fig. 4a. This configuration is similar to that for physisorption of isolated CO_2 on MgO (Fig. 3b). It yields a LDA (PBE) 0.49 (0.08) eV binding energy per CO_2, which is almost identical with that found for isolated CO_2. The predicted herring bone structure and surface CO_2 coverage of $\sim$1/18 Å^{-2} are in good agreement with low temperature LEED experiment[23]. Note that the lateral dimension of the simulation cell used in this work is chosen to be commensurate with the $2\sqrt{2} \times \sqrt{2}$ LEED pattern.

We also consider a structure which has half the CO_2 chemisorbed in the configuration shown in Fig. 3a while the other half has the O-C-O axis aligned along the normal to the MgO surface and coordinated to surface Mg sites via a oxygen atom (Fig. 4b). This structure preserves the experimental coverage of $\sim$ 1/18 Å^{-2} and avoids steric repulsion between neighboring chemisorbed CO_2 molecules. However, the binding energy is only 0.39 (0.06) eV, and is *less* favorable than that found for the physisorbed monolayer (Fig. 4a). In fact, it is less than half that for an isolated chemisorbed CO_2 molecule. The reason for the decrease in binding energy is depolarization. Isolated chemisorbed CO_2 form a substantial dipole moment normal to the MgO surface. When a half layer of CO_2 exist in such a geometry, the induced dipoles on CO_2 electrostatically repel each other. Our calculations explain why the physisorbed monolayer geometry is observed in experiments despite the much larger binding energy for isolated chemisorbed CO_2.

CaO exhibits a 13.3% larger lattice constant. As such, a monolayer CO_2 can chemisorb on CaO (100) without substantial steric repulsion (Fig. 4c). The LDA binding energy is 1.32 eV per CO_2. The physisorbed configuration is bound only by 0.57 eV. Compared to the isolated CO_2 molecule (2.02 eV binding energy), some depolarization effect persists for the chemisorbed monolayer. It is interesting that

the oxides formed by sucessive alkali earth metals in the same main group (Group II) exhibit such dramatically different CO_2 binding behavior due to the difference in their lattice constants.

Our work is a preliminary investigation of the fundamental interactions between CO_2 and oxide materials. Consistent with our previous work[9], we find that CO_2 chemical reactions or chemisorption generally originates from nucleophilic attack on the carbon atom. Many aspects of CO_2 binding on metal oxides remain to be studied. For example, at finite temperature, phase transitions associated with CO_2 coverages on MgO substrates have been observed[24]. The binding energy of water on oxide surfaces is of the same order of magnitude as CO_2 chemisorption. As both flue gases and the atmosphere environment generally contain a higher concentration of moisture than CO_2, coadsorption of these two species need to be examined. Water may decrease the oxide surface available to adsorb CO_2, but may also enhance CO_2 uptake via chemical reactions between adsorbed H_2O and CO_2. Finally, the incorporation of CO_2 into sub-layers of metal oxide materials, not just the top layer, needs to be considered to understand the capture of CO_2 to form bulk metal carbonates.

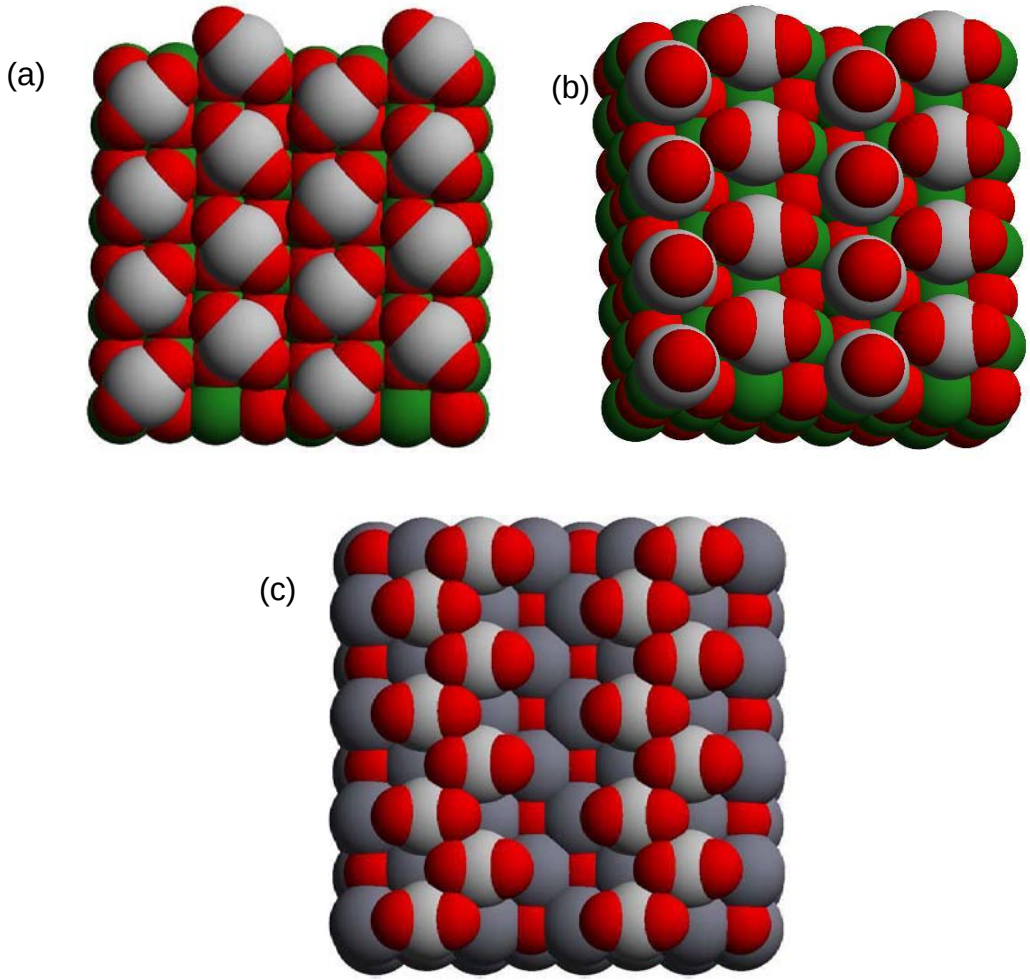

Figure 4. (a) Physisorbed CO_2 monolayer on MgO (100). (b) Half of the CO_2 are chemisorbed while the other half have their molecular axis normal to the MgO surface and one of their oxygen atoms coordinating to the Mg site. (c) Chemisorbed CO_2 monolayer on CaO (100). Green, red, and gray spheres represent Mg/Ca, O, and C, respectively.

4 CO_2 capture in functionalized silica nanopores

A. Introduction

We perform *ab initio* molecular dynamics (AIMD) study of the CO_2 trapping mechanism inside water-filled silica nanopores functionalized with primary amine groups. The initial motivation of examining water-filled nanopores is the potential efficient removal of CO_2 from the flue gas stream via accelerated solvation of CO_2 in confined aqueous media. This hypothesis is based on our previous published work[9]. It is known that that in vacuum (or the "gas phase"), the $CO_2 + OH^- \rightarrow HCO_3^-$ reaction exhibits no activation barrier (Fig. 5a). In liquid water, a 12.1 kcal/mol free energy barrier emerges. This barrier value is reproduced to within 2.4 kcal/mol with AIMD potential of mean force calculations after making corrections with highly accurate quantum chemistry predictions (Fig. 6b)[9]. Inside nanopores, the hydration is impeded, and is intermediate between gas and liquid water environments. Thus the barrier should be reduced from that in water, and the CO_2 capture rate in the confined aqueous media may be enhanced.

However, achievable OH^- concentration may be limited inside nanopores. Our original hypothesis was that hydroxylated silica surfaces, which contain negatively charged SiO^- even at neutral pH, may effectively take the place of OH^- and initate/catalyze the conversion of CO_2 into HCO_3^-. Unfortunately, while the smallest silica fragment $SiO_4H_3^-$ does bind to CO_2, randomly chosen SiO^- in a model silica pore we studied earlier[10] do not – even in the absence of water. When the C atom of a CO_2 molecule is placed next to a SiO^- group on the nanopore interior surface, the system relaxes to a structure where the SiO^- and CO_2 are well-separated. If water were present, H_2O hydrogen bonded to SiO^- would make any reaction with CO_2 even less likely. Thus it unlikely that hydroxylated silica pores will increase CO_2 uptake.

Hence we focus our modeling effort on silica pores functionalized with amine groups. Amine solutions[2] and amine-lined silica nanopores[6] have indeed demonstrated considerable CO_2 capture capability. Our model features $SiCH_2NH_2$ functional groups which replace surface silanol (SiOH) groups in a DFT-optimized silica nanopore structure[10]. This model was originally motivated by synthetic work conducted by Jeff Brinker's research group at Sandia National Laboratories[7].

B. Methods

AIMD simulations apply Density functional theory-predicted forces to propagate Newton's equation of motion and generate trajectories in real time. DFT calculations are performed using the VASP software[17], projected augmented wave (PAW) pseudopotentials[18, 19], the PBE[20] exchange correlation functional, a 400 eV plane wave energy cutoff for wavefunctions, and a 10^{-6} eV convergence criterion. We substitute the deuterium mass for all protons and apply a time step of 0.375 fs. These parameters lead to a total drift in temperature of less than 1 K/ps. In some cases, a harmonic constraint of the form $V(R_{\rm NC}) = A(R - |\mathbf{R}_{\rm N} - \mathbf{R}_{\rm C}|)^2$, with A=6 eV/Å^2, is imposed to accelerate the nucleophilic attack of an amine nitrogen atom on CO_2.

C. Results

In aqueous media, primary amines RNH_2 are known to react with CO_2 to form carbamate anions, $RNHCOO^-$. We first use DFT to model the simplest gas phase reaction of this type, namely CO_2 + NH_3 (Fig. 5a). We find that this reaction not only exhibits a large barrier such that initially placing the N and C atoms close to each other does not lead to a chemical reaction; even if we start with the expected product depicted in Fig. 5b and relax the geometry, the resulting structure is 0.5 eV less stable than the isolated CO_2 and NH_3. This clearly indicates that, unlike OH^-, nucleophilic attack of amine on CO_2 is unfavorable in the gas phase, and that the CO_2 capture capability of amine groups is due to the co-presence of water molecules.

Next, we consider a 1.2 nm diameter silica nanopore model in which 11 out of the 38 SiOH groups in the interior surface have been replaced with $SiCH_2N_2$ groups[10]. The 15.3 Å long unit cell is filled with 35 water molecules. If the pore were a flat amine-functionalized surface in the presence of water, all surface NH_2 functional groups will abstract a proton from a surface SiOH group due to the relative pK_a of the respective species. If this were true of our pore model, the 11 NH_2 will turn into 11 NH_3^+ groups, each of which requires three hydrogen bonds to become stabilized, but there are only 35 water molecules in the nanopore to provide hydration. This prompted us to investigate the surface chemistry of nanopores so functionalized using AIMD[10]. We found that some of the NH_3^+ stabilitzation is provided by surface SiO^- groups. Nevertheless, two O(10) ps AIMD simulation runs from different initial configurations both show that 20% of amine groups remain NH_2[10]. See Fig. 5c.

In this LDRD, we extend this previous work to examine chemical reactions with CO_2. CO_2 should not react with NH_3^+. However, it may react with the 20% of amine

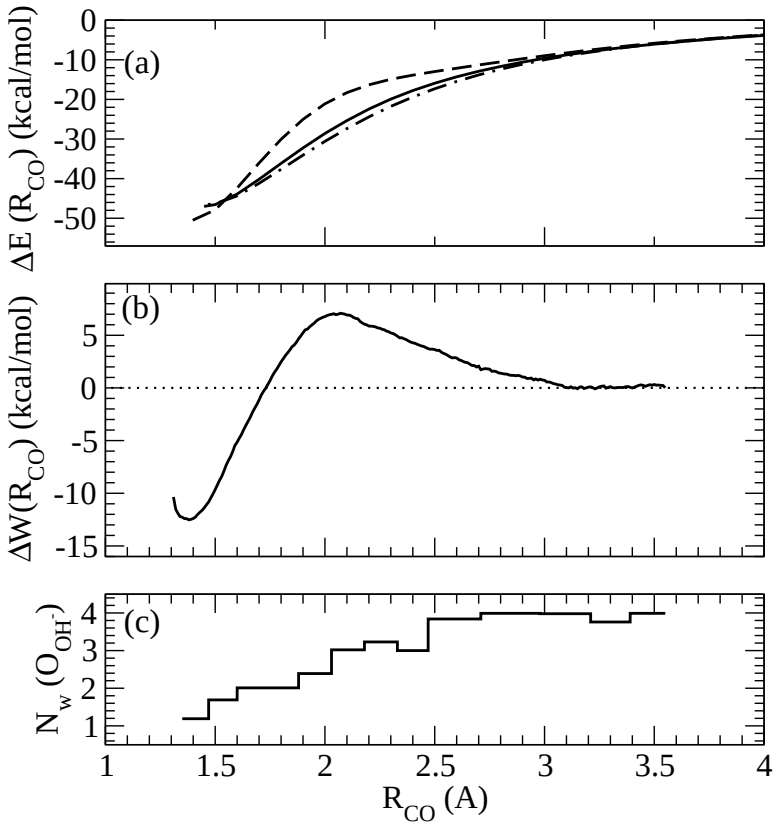

Figure 5. (a) Energy along CO_2 + OH^- reaction coordinate at T=0 K, using Hartree-Fock, MP2, and PBE methods. (b) Free energy along this reaction coordinate at T=300 K. Zero point and entropic corrections have not been added. (c) Hydration number (N_w) for the OH^- ion, which becomes part of the HCO_3^- molecule as $R_{\rm CO}$, the reaction coordinate, decreases.

groups that have remained NH_2 via nucleophilic attack of the nitrogen atom on the CO_2 carbon. The nanoconfinement geometry thus appears to aid CO_2 capture by inducing some NH_2 groups to remain as primary amine in water instead of converting all of them into ammonium groups. So we next introduce carbon dioxide by replacing a H_2O hydrogen bonded to a NH_2 group with a CO_2 molecule (Fig. 5d), and intiate the AIMD trajectory. Within 0.7 ps, the CO_2 spontaneous reacts with the NH_2 group to form a zwitterionic $RNH_2^+COO^-$ complex stabilized by water. See Fig. 5e. The C-N bond length fluctuates between 1.4 and 1.6 Å. This is encouraging because this spontaneously formed complex appears metastable, and may already be sufficiently strongly bound for CO_2 capture. Detailed AIMD potential of mean force calculations are required to predict the formation free energy of this complex to verify the utility of narrow functionalized nanopores in CO_2 capture applications.

Next, we apply a harmonic potential to shorten the amine-CO_2 N-C bond to an average of 1.3 Angstrom to determine if additional reactions can occur. In sub-picosecond time scales, we find that one of the protons on the N atom dissociates, and then a NH_2COOH ("carbamic acid") complex is formed via proton transfer from the NH_2 to the -COO^- through proton hopping (the Grotthus mechnism) via a two-H_2O bridge. See Fig. 5f. This product appears more stable than the zwitterion (Fig. 5e). Again, the free energy gain and the barrier associated with this reaction need to be determined using systematic AIMD potential of mean force calculations.

D. Conclusions

In conclusion, AIMD simulations have revealed novel mechanisms associated with CO_2 capture using water-filled, amine-group lined silica nanopores. Several experimental groups at Sandia are exploring this amine functional group route to develop nanostructured CO_2-capture platforms. This exploratory modeling study has identified the key AIMD potential of mean force calculations that should be performed in the future, and it has the potential to assist rational design of more efficient CO_2 capture materials.

Our AIMD study is also closely related to theoretical studies being pursued by one of the team members (KL) and his academic collaborators. These include the condensation of amino acids to form peptide catalyzed by minerals at high temperature and pressure in a proposed "origins of life" scenario (Alenka Luzar's research group at Virginia Commonwealth University, potential NASA funding); the hydrolysis of amides in water, pertinent to many biological functions (Ken Merz's research group at the University of Florida); and continued study of other CO_2 reactions in water

(Ira Kurtz at the University of California at Los Angeles). A common thread to these studies is the modeling of chemical reaction mechanisms that involve multiple steps. The recently developed metadynamics method[26] may be a viable technique to tackle the complexity inherent to such chemical reactions.

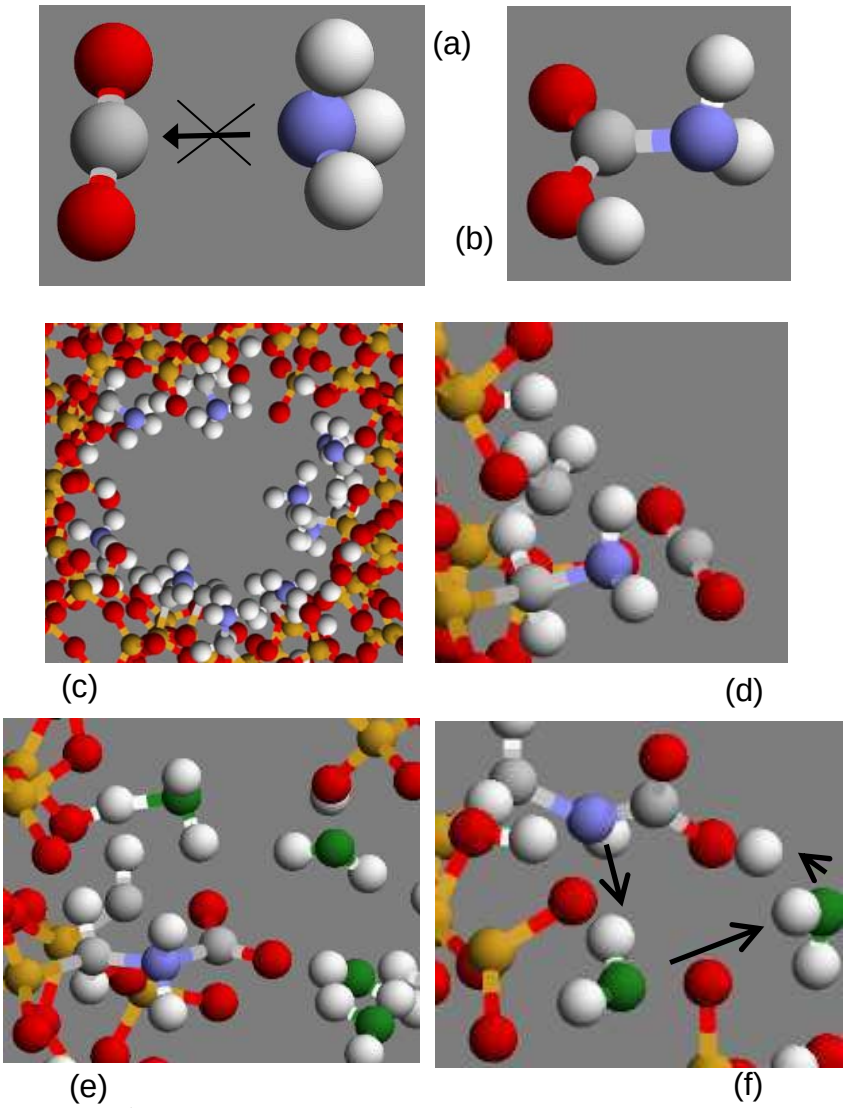

Figure 6. (a) CO_2 does not spontaneously react with NH_3. (b) The product NH_2COOH is metastable. (c) CH_2NH_2 functionalized silica nanopore filled with water. (d) t=0 ps: CO_2 placed near an NH_2 group. (e) t=0.7 ps: spontaneous formation of $CH_2NH_2^+COO^-$. (f) With a distance constraint, $CH_2NHCOOH$ forms via proton transfer over a 2-H_2O bridge. Yellow, red, gray, blue, and white spheres represent Si, O, C, N, and H atoms, respectively. In panel (f), the water oxygen atoms are colored in green. All other water molecules in the water-filled nanopore in panels (c)-(f) are removed for clarity reasons.

References

[1] IPCC Special Report on Carbon Dioxide Capture and Storage: http://www.ipcc.ch/activity/srccs/index.htm

[2] D. Saylik, M. J. Horvath, P. S. Elmes, and W. R. Jackson, J. Org. Chem. **64**, 3940 (1999).

[3] G. M. Bond *et al.*, Energy & Fuels **15**, 309 (2001), and references therein.

[4] Carbon Dioxide Sequestration: State of the Science (DOE, Washington), 1999, http://www.fe.doe.gov/programs/sequestration/capture/index.htm

[5] R. Baciocchi, G. Storti, and M Mazzotti, Chem. Engr. Processing **45**, 1047 (2006).

[6] M. L. Gray, Y. Soong, K. J. Champagne, H. Pennline, J. P. Baltrus, R. W. Stevens, R. Khatri, S. S. C. Chuang, and T. Filburn, Fuel Processing Technology **86**, 1449 (2005).

[7] N.-G. Liu, R. A. Assink, B. Smarsly, and C. J. Brinker, Chem. Commun. **10**, 1146 (2003).

[8] LDRD funded from 2006-2008, entitled "Exploiting Interfacial Water Properties for Desalination and Purification Applications," (Randy Cygan, Tina Nenoff, Peter Feibelman, Jeff Brinker, and Bruce Bunker as P.I.).

[9] K. Leung, I. M. B. Nielsen, and I. Kurtz, J. Phys. Chem. B **111**, 4453 (2007).

[10] K. Leung, S. B. Rempe, and C. D. Lorenz, Phys. Rev. Lett. **96**, 095504 (2006).

[11] Currently funded LDRD entitled "Direct Approaches for Recycling Carbon Dioxide into Synthetic Fuel," (James Miller as P.I.).

[12] T.M. Nenoff, J. D. Pless, E. Michaels, and M. L. F. Phillips, Chem. Materials **17**, 950 (2005).

[13] X. H. Gu, J. H. Dong, and T. M. Nenoff, Ind. Eng. Chem. Res. **44**, 937 (2005).

[14] Z. Tang, J. H. Dong, and T. M. Nenoff, J. Memb. Sci. (2008, in prep).

[15] B. Feng, H. An, and E. Tan, Energy & Fuels **21**, 426 (2007).

[16] B. Feng, W. Q. Liu, X. Li, and H. An, Energy & Fuels **20**, 2417 (2006).

[17] G. Kresse and J. Furthmüller, Phys. Rev. B **54**, 11169 (1996), Comput. Mater. Sci. **6**, 15 (1996).

[18] P. E. Blöchl, Phys. Rev. B, **50**, 17953 (1994).

[19] The VASP implementation is discussed in G. Kresse and D. Joubert, Phys. Rev. B **59**, 1758 (1999).

[20] J. P. Perdew, K. Burke, K. M. Ernzerhof, Phys. Rev. Lett. **77**, 3865 (1996).

[21] W. F. Schneider, J. Phys. Chem. B **108**, 273 (2004).

[22] Pacchioni *et al.*, J. Am. Chem. Soc. **116**, 10152 (1994).

[23] Panetta *et al.*, J. Phys. France **1**, 905 (1994).

[24] C. D. Daub, G. N. Patey, D. B. Jack, and A. K. Sallabi, J. Chem. Phys. **124**, 114706 (2006), and references therein.

[25] D. E. Penny and T. J. Ritter, J. Chem. Soc. Faraday Trans. 1 **79**, 2103 (1983).

[26] See, e.g., A. Laio, A. Rodriguez-Fortea, F. Luigi Gervasio, M. Ceccarelli, and M. Parrinello, J. Phys. Chem. B **109**, 6714 (2005).

DISTRIBUTION:

1	MS 1415	Kevin Leung, 1114
1	MS 1415	Tina M. Nenoff, 1114
1	MS 0745	Louise J. Criscenti, 6316
1	MS 1415	Carlos Gutierrez, 1114
1	MS 1415	Ida Nielsen, 8961
1	MS 0734	Ellen B. Stechel, 06330
1	MS 0734	Timothy N. Lambert, 06338
1	MS 0734	Chad L. Staiger, 06338
1	MS 9536	Technical Library, 0899 (electronic copy)
1	MS 0123	D.L. Chavez, 1011